View metadata, citation and similar papers at core.ac.uk
brought to you by CORE
provided by Repositorio da Universidade da Coruña

BEAM RECONFIGURATION OF LINEAR ARRAYS BY USING PARASITIC ELEMENTS

J. A. Rodríguez[(1)], A. Trastoy [(1)], Julio C. Brégains[(1)], F. Ares[(1)] and G. Franceschetti[(2)]

[(1)]University of Santiago de Compostela, Grupo de Sistemas Radiantes, Dpto. Física Aplicada, Facultad de Física, 15782 Santiago de Compostela, Spain. Email: faares@usc.es

[(2)] Dept. of Electronic Engineering, University of Naples (Italy) and UCLA (USA) 80125 Napoli (Italy). Email: gfrance@unina.it

ABSTRACT

An innovative method for linear arrays beam reconfiguration is presented. This pattern reconfigurability is achieved by a mechanical displacement of a parasitic array located in front of an active one. Two worked out examples that use parallel dipoles are presented.

1. INTRODUCTION

Antenna array pattern reconfiguration is usually achieved by changing the relative amplitudes and/or phases of the excitations of its radiating elements. However, this approach often requires the design and realization of beam-forming networks of considerable complexity [1-5]. In this paper we explore an alternative approach: the mechanical displacement of a parasitic array in front of an active one. The currents in the driven and parasitic elements are determined via their self and mutual impedances: their design leads to the desired radiation pattern change, thus achieving the antenna system reconfigurability. In the following, we apply the presented idea to an interesting

case: the possibility of switching the power pattern from a pencil to a flat-topped broadside beam. However, this is only an example: the proposed technique may be applied to any other desired radiation pattern reconfiguration and may be of interest, in view of its simplicity, to several applications that do not require real time reconfigurability.

2. PRESENTATION OF THE METHOD IN THE FRAME OF A CASE STUDY

Consider an antenna system composed by two arrays: *N* actively radiating dipoles parallel to the *z* axis and equispaced along the *x* axis, together with *M* similarly oriented parasitic dipoles placed on a line parallel to the same *x* axis (Fig. 1). The latter array is divided into two halves: we show in the following that a pencil beam (F_A) is generated, when the distance Δx between them is properly increased, whereas a flat-topped beam (F_B) is achieved when Δx is shortened, see Fig.2. As a matter of fact, the spacing change from Δx_A to Δx_B modifies the positions of the parasitic elements: accordingly, the currents of both driven and parasitic dipoles are modified due to the mutual coupling. Computation of the radiation diagram requires evaluation of the currents distribution. This can be accomplished via the matrix equation $[V]=[Z][I] \Rightarrow [I]=[Z]^{-1}[V]$, where $[V]$ is the (known) vector of the complex voltages applied to the driven and parasitic elements (obviously $V_m = 0$ for the parasitic elements), $[I]$ the (unknown) vector of the relative complex excitations of both the driven and parasitic elements, and $[Z]$ the impedance matrix. The entries of the latter are calculated by means of the expression developed by King et al. [6] as far as the self-impedances Z_{nn} of center-fed cylindrical dipoles are concerned, whereas the expression given in [7] is applied to calculate the mutual impedances Z_{mn}.

The resulting currents distribution depends on the complex voltages $\{V_1, V_2, ..., V_N\}$ applied to the driven elements, on the distances Δx between the two halves of the parasitic array and on the

spacing Δy between the two arrays, see Fig.2. All these elements are the design parameters to compute the radiation diagram $F(\theta,\phi)$ of the considered antenna system by following the conventional approach:

$$F(\theta,\phi)=\sum_{n=1}^{N} I_n \exp\{jkx_n \sin\theta\cos\phi\}\cdot f_n(\theta)+\sum_{m=1}^{M} I'_m \exp\{jk\sin\theta(x'_m\cos\phi+\Delta y\sin\phi)\}\cdot f_m(\theta) \qquad (1)$$

with the *n*-th actively radiating and the *m*-th parasitic elements located at $(x_n,0,0)$ and $(x'_m,\Delta y,0)$, respectively, see Fig. 1, and $f_i(\theta)$ being the element factor of dipole *i*, see [7]. The lengths of each driven and parasitic dipoles may be also used as design parameters.

For any prescribed radiation diagram, the simulated annealing [8] is used to find the values of the design parameters. This method is capable of attaining additional desired features: in Sect. 3, the minimization of the maximum variation of the active impedances of driven elements, $|\Delta \mathrm{Re}(Z_n^A)|_{\max}$ and $|\Delta \mathrm{Im}(Z_n^A)|_{\max}$, when the antenna switches between patterns, is implemented.

When a ground plane is placed behind the driven array (y<0) to concentrate the radiation in only one hemisphere of the space, the considerations derived from the image principle –and presented in [7]– are applied to the self and mutual impedances evaluation. The modified expression of the element factor is also obtained from [7].

3. NUMERICAL EXAMPLES

As an example, an antenna composed by a 21-element actively radiating array and a 14 parasitic-element array is considered: we want to switch its radiation pattern from a pencil to a flat-topped beam. To reduce the number of variables in the optimization process, both the driven and the parasitic arrays are supposed to be symmetric with respect to their corresponding centers, and such symmetry is concerned to their lengths, voltages and positions as well.

Results of the design are provided in Fig. 3, where the obtained radiation patterns are depicted:

i) a pencil beam with -20.0 dB sidelobe level (SLL) that is radiated by the antenna when $\Delta x_A = 11\lambda$;

ii) a flat-topped beam pattern with 44.2 deg. beamwidth measured at -3 dB, ±0.25 dB of ripple and SLL = -20.0 dB that is radiated by the same antenna when $\Delta x_B = 2.8\lambda$.

In both cases the parasitic array is located $\Delta y = 0.15\lambda$ apart from the driven array. The maximum variation of the active impedance of driven elements obtained in this case is $|\Delta \mathrm{Re}(Z_n^A)|_{\max} = 43.2\Omega$ and $|\Delta \mathrm{Im}(Z_n^A)|_{\max} = 66.08\Omega$. The interelement distance of the dipoles is equal to 0.5λ.

In a new optimization (whose data are not referred in the paper) the maximum variation of the active resistance can be greatly reduced to $|\Delta \mathrm{Re}(Z_n^A)|_{\max} = 7.86\,\Omega$, at the expense of increasing the variation of active reactance $|\Delta \mathrm{Im}(Z_n^A)|_{\max} = 103.36\,\Omega$ and slightly reducing the performance of the patterns (a pencil beam with -18.9 dB sidelobe level and a flat-topped beam with -18.9 dB sidelobe level and a ripple of ±0.55 dB).

If a ground plane is located $\lambda/4$ behind the driven array, similar results are obtained (see Fig. 4):

i) a pencil beam with -19.5 dB of SLL that is radiated by the antenna when $\Delta x_A = 12.7\lambda$;

ii) a flat-topped pattern with 44.2 deg. beamwidth measured at -3 dB, ±0.35 dB ripple and SLL= -19.7 dB that is radiated by the same antenna when $\Delta x_B = 2.7\lambda$.

In both cases, $\Delta y = 0.20\lambda$ and the interelement distance 0.5λ as before. The presence of the ground plane significantly increased the variation of active impedances to the values $|\Delta \mathrm{Re}(Z_n^A)|_{\max} = 456\Omega$ and $|\Delta \mathrm{Im}(Z_n^A)|_{\max} = 342.7\Omega$: as above, this feature can be improved at the expense of reducing the performance of the obtained patterns.

4. CONCLUSIONS

A study on the use of parasitic arrays to reconfigure the beam radiated by a linear array, realized by means of a mechanical displacement of parasitic elements, has been presented. Examples have been shown to illustrate the patterns obtained with this approach. It is explicitly noted the simple mechanical possible implementation of the system: a rail and a micro-step motor. By this means, a gradual transition from the pencil to the flat-topped pattern can be obtained.

We are currently extending this method by using a moments-based commercial software tool that is capable of taking into account dielectric substrates, more complicated current distributions on the actively radiating elements, frequency response, etc. We believe that the presented technique can be extended to planar and conformal arrays and to reflectors (by inserting parasitic “wings” into the system). It can be also applied to horns or small arrays illuminating a larger parasitic array to obtain a narrow pencil beam using a small (in terms of wavelengths) actively radiating antenna, so that only few elements of the overall system are driven.

5. REFERENCES

[1] BUCCI, O. M., MAZZARELLA, G., AND PANARIELLO, G., 'Reconfigurable arrays by phase-only control', *IEEE Trans. Antennas Propagat.*, 1991, **39** (7), pp. 919-925.

[2] DÜRR, M., TRASTOY, A., AND ARES, F., 'Multiple pattern linear antenna arrays with single prefixed amplitude distributions: modified Woodward-Lawson synthesis', 2000, *Electron. Lett.*, **36** (16), pp. 1345-1346.

[3] DÍAZ, X., RODRÍGUEZ, J. A., ARES, F., AND MORENO, E., 'Design of phase-differentiated multiple-pattern antenna arrays', *Microwave Opt. Technology Lett.* , 2000, **16** (1) pp. 52-53.

[4] BRÉGAINS, J. C., TRASTOY, A., ARES, F., AND MORENO, E., 'Synthesis of multiple-pattern planar antenna arrays with single prefixed or jointly optimised amplitude distributions', *Microwave Opt. Technology Lett.*, 2002, **32** (1), pp. 74-78.

[5] TRASTOY, A., RAHMAT-SAMII, Y., ARES, F., AND MORENO, E., 'Two pattern linear array antenna: synthesis and analysis of tolerance', *IEE Proc., Microw. Antennas Propagat.*, 2004, **151** (2), pp. 127-130.

[6] KING, R. W. P., ARONSON, E. A., AND HARRISON, C. W., 'Determination of the Admittance and Effective Length of Cylindrical Antennas', *Radio Science*, 1966, **1**, pp. 835-850.

[7] ELLIOTT, R. S., *Antenna Theory and Design. Revised Edition*, 2003, John Wiley and Sons, Inc., Hoboken, New Jersey, USA.

[8] PRESS, W. H., FLANNERY, B. P., TEUKOLSKY, S. A., AND VETTERLING W. T., *Numerical Recipes in C*, 1992, Cambridge University Press, New York, USA.

CAPTIONS OF FIGURES

Fig. 1. Geometry of the driven and parasitic arrays of dipoles. For reference, a spherical system of coordinates (θ,ϕ) is also depicted, for subsequent computation of the radiated field.

Fig.2. Location of the parasitic elements when a) a pencil beam is radiated (F_A), b) when a flat topped beam is radiated (F_B).

Fig. 3. Patterns radiated in the $\theta=\pi/2$ plane by a 21-element linear array of dipoles with $\Delta x_A = 11\lambda$ (solid line) or $\Delta x_B = 2.8\lambda$ (dashed line). No ground plane is considered.

Fig. 4. Patterns radiated in the $\theta=\pi/2$ plane by a 21-element linear array of dipoles with $\Delta x_A=12.7\lambda$ (solid line) or $\Delta x_B=2.7\lambda$ (dashed line). A ground plane is located $\lambda/4$ behind the driven array.

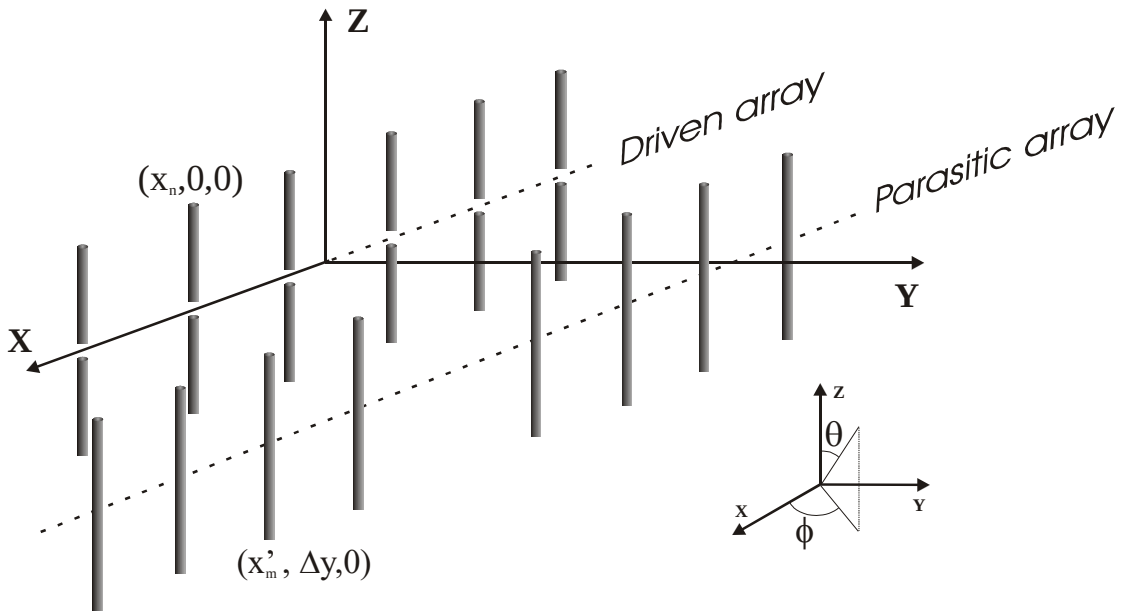

Figure 1

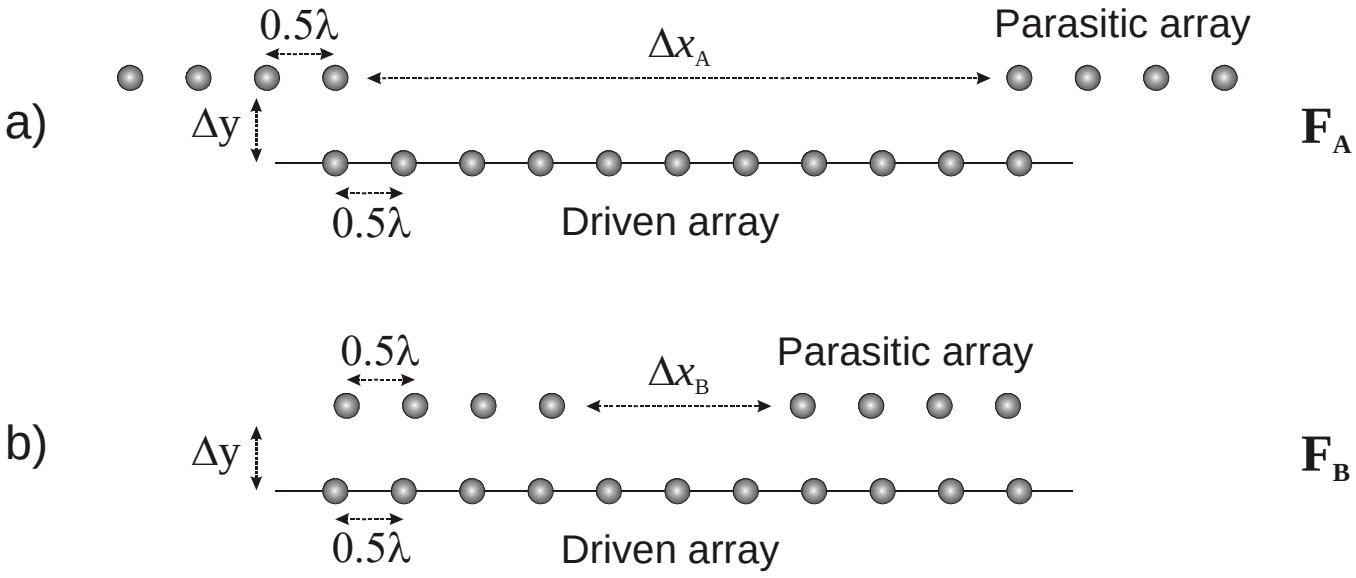

Figure 2

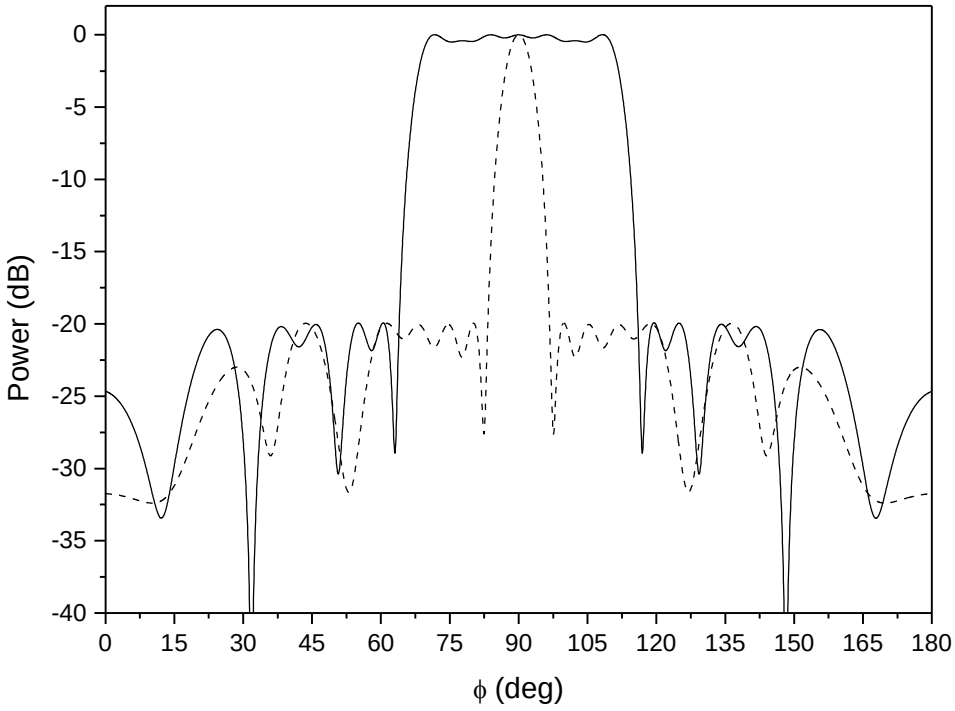

Figure 3

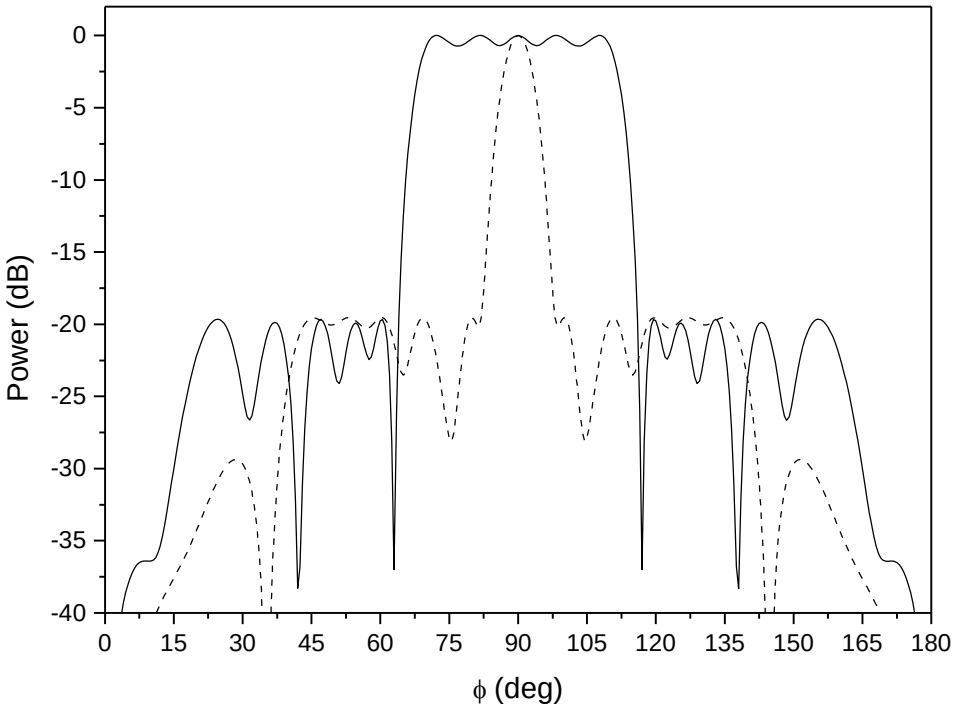

Figure 4